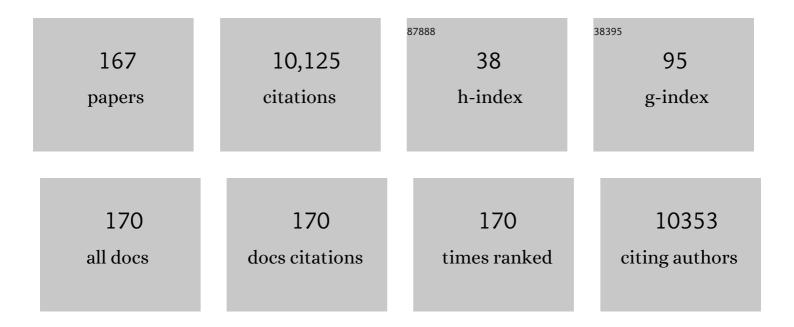
List of Publications by Year in descending order

Source: https://exaly.com/author-pdf/5771499/publications.pdf Version: 2024-02-01



IDENE RUMAT

#	Article	IF	CITATIONS
1	A Guide to ComBat Harmonization of Imaging Biomarkers in Multicenter Studies. Journal of Nuclear Medicine, 2022, 63, 172-179.	5.0	96
2	An [18F]FDG-PET/CT deep learning method for fully automated detection of pathological mediastinal lymph nodes in lung cancer patients. European Journal of Nuclear Medicine and Molecular Imaging, 2022, 49, 881-888.	6.4	15
3	Nuclear Medicine and Artificial Intelligence: Best Practices for Algorithm Development. Journal of Nuclear Medicine, 2022, 63, 500-510.	5.0	43
4	Clever Hans effect found in a widely used brain tumour MRI dataset. Medical Image Analysis, 2022, 77, 102368.	11.6	14
5	Voxelâ€wise supervised analysis of tumors with multimodal engineered features to highlight interpretable biological patterns. Medical Physics, 2022, 49, 3816-3829.	3.0	12
6	Effects of Tracer Uptake Time in Non–Small Cell Lung Cancer <sup>18</sup> F-FDG PET Radiomics. Journal of Nuclear Medicine, 2022, 63, 919-924.	5.0	6
7	Prognostic value of lesion dissemination in doxorubicin, bleomycin, vinblastine, and dacarbazineâ€treated, interimPETâ€negative classical Hodgkin Lymphoma patients: A radioâ€genomic study. Hematological Oncology, 2022, 40, 645-657.	1.7	19
8	<sup>18</sup> F-FDG PET Maximum-Intensity Projections and Artificial Intelligence: A Win-Win Combination to Easily Measure Prognostic Biomarkers in DLBCL Patients. Journal of Nuclear Medicine, 2022, 63, 1925-1932.	5.0	18
9	Deep-Learning <sup>18</sup> F-FDG Uptake Classification Enables Total Metabolic Tumor Volume Estimation in Diffuse Large B-Cell Lymphoma. Journal of Nuclear Medicine, 2021, 62, 30-36.	5.0	75
10	How can we combat multicenter variability in MR radiomics? Validation of a correction procedure. European Radiology, 2021, 31, 2272-2280.	4.5	93
11	A radiomics pipeline dedicated to Breast MRI: validation on a multi-scanner phantom study. Magnetic Resonance Materials in Physics, Biology, and Medicine, 2021, 34, 355-366.	2.0	20
12	lrène Buvat and Ken Herrmann Talk with Alexander Stremitzer, Kevin Tobia, and Aileen Nielsen. Journal of Nuclear Medicine, 2021, 62, 3-5.	5.0	5
13	Potentials and caveats of Al in hybrid imaging. Methods, 2021, 188, 4-19.	3.8	12
14	Just another "Clever Hans� Neural networks and FDG PET-CT to predict the outcome of patients with breast cancer. European Journal of Nuclear Medicine and Molecular Imaging, 2021, 48, 3141-3150.	6.4	23
15	Total metabolic tumor volume and spleen metabolism on baseline [18F]-FDG PET/CT as independent prognostic biomarkers of recurrence in resected breast cancer. European Journal of Nuclear Medicine and Molecular Imaging, 2021, 48, 3560-3570.	6.4	14
16	The T.R.U.E. Checklist for Identifying Impactful Artificial Intelligence–Based Findings in Nuclear Medicine: Is It True? Is It Reproducible? Is It Useful? Is It Explainable?. Journal of Nuclear Medicine, 2021, 62, 752-754.	5.0	13
17	New PET technologies – embracing progress and pushing the limits. European Journal of Nuclear Medicine and Molecular Imaging, 2021, 48, 2711-2726.	6.4	35
18	Comment on Ibrahim et al. The Effects of In-Plane Spatial Resolution on CT-Based Radiomic Features' Stability with and without ComBat Harmonization. Cancers 2021, 13, 1848. Cancers, 2021, 13, 3037.	3.7	8

#	Article	IF	CITATIONS
19	New Approaches in Characterization of Lesions Dissemination in DLBCL Patients on Baseline PET/CT. Cancers, 2021, 13, 3998.	3.7	12
20	Radiomics in PET Imaging. PET Clinics, 2021, 16, 597-612.	3.0	40
21	Quantitative Image Analysis in Tomography. , 2021, , 1407-1429.		0
22	<sup>18</sup> F-FDG PET Dissemination Features in Diffuse Large B-Cell Lymphoma Are Predictive of Outcome. Journal of Nuclear Medicine, 2020, 61, 40-45.	5.0	109
23	The Image Biomarker Standardization Initiative: Standardized Quantitative Radiomics for High-Throughput Image-based Phenotyping. Radiology, 2020, 295, 328-338.	7.3	1,869
24	Longitudinal mouse-PET imaging: a reliable method for estimating binding parameters without a reference region or blood sampling. European Journal of Nuclear Medicine and Molecular Imaging, 2020, 47, 2589-2601.	6.4	7
25	Correction for Magnetic Field Inhomogeneities and Normalization of Voxel Values Are Needed to Better Reveal the Potential of MR Radiomic Features in Lung Cancer. Frontiers in Oncology, 2020, 10, 43.	2.8	17
26	The Dark Side of Radiomics: On the Paramount Importance of Publishing Negative Results. Journal of Nuclear Medicine, 2019, 60, 1543-1544.	5.0	58
27	Validation of A Method to Compensate Multicenter Effects Affecting CT Radiomics. Radiology, 2019, 291, 53-59.	7.3	257
28	A downsampling strategy to assess the predictive value of radiomic features. Scientific Reports, 2019, 9, 17869.	3.3	5
29	Longitudinal positron emission tomography imaging of glial cell activation in a mouse model of mesial temporal lobe epilepsy: Toward identification of optimal treatment windows. Epilepsia, 2018, 59, 1234-1244.	5.1	36
30	Is there an optimal method for measuring baseline metabolic tumor volume in diffuse large B cell lymphoma?. European Journal of Nuclear Medicine and Molecular Imaging, 2018, 45, 1463-1464.	6.4	19
31	Computation of reliable textural indices from multimodal brain MRI: suggestions based on a study of patients with diffuse intrinsic pontine glioma. Physics in Medicine and Biology, 2018, 63, 105003.	3.0	32
32	A Postreconstruction Harmonization Method for Multicenter Radiomic Studies in PET. Journal of Nuclear Medicine, 2018, 59, 1321-1328.	5.0	250
33	Imaging the neuroimmune response to alcohol exposure in adolescent baboons: a TSPO PET study using <sup>18</sup> Fâ€DPAâ€714. Addiction Biology, 2018, 23, 1000-1009.	2.6	23
34	A score combining baseline neutrophilia and primary tumor SUVpeak measured from FDG PET is associated with outcome in locally advanced cervical cancer. European Journal of Nuclear Medicine and Molecular Imaging, 2018, 45, 187-195.	6.4	25
35	Interval-based reconstruction for uncertainty quantification in PET. Physics in Medicine and Biology, 2018, 63, 035014.	3.0	10
36	Impact of Endothelial 18-kDa Translocator Protein on the Quantification of <sup>18</sup> F-DPA-714. Journal of Nuclear Medicine, 2018, 59, 307-314.	5.0	52

#	Article	IF	CITATIONS
37	Physical blood-brain barrier disruption induced by focused ultrasound does not overcome the transporter-mediated efflux of erlotinib. Journal of Controlled Release, 2018, 292, 210-220.	9.9	37
38	P-Glycoprotein (ABCB1) Inhibits the Influx and Increases the Efflux of <sup>11</sup> C-Metoclopramide Across the Blood–Brain Barrier: A PET Study on Nonhuman Primates. Journal of Nuclear Medicine, 2018, 59, 1609-1615.	5.0	39
39	Radiomics in Nuclear Medicine Applied to Radiation Therapy: Methods, Pitfalls, and Challenges. International Journal of Radiation Oncology Biology Physics, 2018, 102, 1117-1142.	0.8	86
40	LIFEx: A Freeware for Radiomic Feature Calculation in Multimodality Imaging to Accelerate Advances in the Characterization of Tumor Heterogeneity. Cancer Research, 2018, 78, 4786-4789.	0.9	717
41	Influence of age on radiomic features in 18F-FDG PET in normal breast tissue and in breast cancer tumors. Oncotarget, 2018, 9, 30855-30868.	1.8	11
42	Acute Morphine Exposure Increases the Brain Distribution of [ <sup>18</sup> F]DPA-714, a PET Biomarker of Glial Activation in Nonhuman Primates. International Journal of Neuropsychopharmacology, 2017, 20, pyw077.	2.1	16
43	Multi-centre evaluation of accuracy and reproducibility of planar and SPECT image quantification: An IAEA phantom study. Zeitschrift Fur Medizinische Physik, 2017, 27, 98-112.	1.5	35
44	Evaluation of TSPO PET imaging, a marker of glial activation, to study the neuroimmune footprints of morphine exposure and withdrawal. Drug and Alcohol Dependence, 2017, 170, 43-50.	3.2	13
45	Report of the 6th International Workshop on PET in lymphoma. Leukemia and Lymphoma, 2017, 58, 2298-2303.	1.3	21
46	Imaging Probes and Modalities for the Study of Solute Carrier O (SLCO)-Transport Function InÂVivo. Journal of Pharmaceutical Sciences, 2017, 106, 2335-2344.	3.3	14
47	A Score Combining SUV peak of the Primary Tumor Computed on Pretreatment FDG-PET Scans and Neutrophilia Predicts Outcome in Locally Advanced Cervical Cancer. International Journal of Radiation Oncology Biology Physics, 2017, 99, E310-E311.	0.8	1
48	Subject-specific bone attenuation correction for brain PET/MR: can ZTE-MRI substitute CT scan accurately?. Physics in Medicine and Biology, 2017, 62, 7814-7832.	3.0	30
49	Joint prediction of multiple scores captures better individual traits from brain images. NeuroImage, 2017, 158, 145-154.	4.2	35
50	Understanding Changes in Tumor Texture Indices in PET: A Comparison Between Visual Assessment and Index Values in Simulated and Patient Data. Journal of Nuclear Medicine, 2017, 58, 387-392.	5.0	86
51	Strategies to Inhibit ABCB1- and ABCG2-Mediated Efflux Transport of Erlotinib at the Blood–Brain Barrier: A PET Study on Nonhuman Primates. Journal of Nuclear Medicine, 2017, 58, 117-122.	5.0	43
52	Brain Lesion Detection in 3D PET Images Using Max-Trees and a New Spatial Context Criterion. Lecture Notes in Computer Science, 2017, , 455-466.	1.3	5
53	Prediction of cervical cancer recurrence using textural features extracted from 18F-FDG PET images acquired with different scanners. Oncotarget, 2017, 8, 43169-43179.	1.8	100
54	Methodologies for quantitative SPECT. Imaging in Medical Diagnosis and Therapy, 2017, , 195-210.	0.0	0

#	Article	IF	CITATIONS
55	A <scp>gate</scp> evaluation of the sources of error in quantitative <sup>90</sup> Y PET. Medical Physics, 2016, 43, 5320-5329.	3.0	13
56	Redesign of the GATE PET coincidence sorter. Physics in Medicine and Biology, 2016, 61, N522-N531.	3.0	15
57	In Regard to Mattonen etÂal. International Journal of Radiation Oncology Biology Physics, 2016, 95, 1544-1545.	0.8	17
58	Multiscale Texture Analysis: From <sup>18</sup> F-FDG PET Images to Histologic Images. Journal of Nuclear Medicine, 2016, 57, 1823-1828.	5.0	56
59	Imaging the Impact of the P-Glycoprotein (ABCB1) Function on the Brain Kinetics of Metoclopramide. Journal of Nuclear Medicine, 2016, 57, 309-314.	5.0	47
60	Using simulations of the detector performance for enhanced image reconstruction in molecular imaging. Nuclear Instruments and Methods in Physics Research, Section A: Accelerators, Spectrometers, Detectors and Associated Equipment, 2016, 809, 89-95.	1.6	0
61	18F-FDG PET-Derived Textural Indices Reflect Tissue-Specific Uptake Pattern in Non-Small Cell Lung Cancer. PLoS ONE, 2015, 10, e0145063.	2.5	115
62	Improved Estimation of Cardiac Function Parameters Using a Combination of Independent Automated Segmentation Results in Cardiovascular Magnetic Resonance Imaging. PLoS ONE, 2015, 10, e0135715.	2.5	11
63	Variability and Uncertainty of <sup>18</sup> F-FDG PET Imaging Protocols for Assessing Inflammation in Atherosclerosis: Suggestions for Improvement. Journal of Nuclear Medicine, 2015, 56, 552-559.	5.0	89
64	3D+t segmentation of PET images using spectral clustering. , 2015, , .		0
65	Apport de l'imagerie hybride TEP-IRM pour la quantification en TEP. Medecine Nucleaire, 2015, 39, 291-292.	0.2	0
66	Unsupervised Spectral Clustering for Segmentation of Dynamic PET Images. IEEE Transactions on Nuclear Science, 2015, 62, 840-850.	2.0	16
67	Tumor Texture Analysis in PET: Where Do We Stand?. Journal of Nuclear Medicine, 2015, 56, 1642-1644.	5.0	93
68	Monitoring therapeutic efficacy of sunitinib using [18F]FDG and [18F]FMISO PET in an immunocompetent model of luminal B (HER2-positive)-type mammary carcinoma. BMC Cancer, 2015, 15, 534.	2.6	15
69	Monte-Carlo simulations of clinically realistic respiratory gated 18F-FDG PET: Application to lesion detectability and volume measurements. Computer Methods and Programs in Biomedicine, 2015, 118, 84-93.	4.7	7
70	Fluorine 18 Fluorodeoxyglucose PET/CT Volume-based Indices in Locally Advanced Non–Small Cell Lung Cancer: Prediction of Residual Viable Tumor after Induction Chemotherapy. Radiology, 2014, 272, 875-884.	7.3	20
71	Extension of the GATE Monte-Carlo simulation package to model bioluminescence and fluorescence imaging. Journal of Biomedical Optics, 2014, 19, 026004.	2.6	28
72	Monitoring tumour response during chemo-radiotherapy: a parametric method using FDG-PET/CT images in patients with oesophageal cancer. EJNMMI Research, 2014, 4, 12.	2.5	19

#	Article	IF	CITATIONS
73	A review of the use and potential of the GATE Monte Carlo simulation code for radiation therapy and dosimetry applications. Medical Physics, 2014, 41, 064301.	3.0	332
74	Variational Segmentation of Vector-Valued Images With Gradient Vector Flow. IEEE Transactions on Image Processing, 2014, 23, 4773-4785.	9.8	26
75	Tumor Texture Analysis in <sup>18</sup> F-FDG PET: Relationships Between Texture Parameters, Histogram Indices, Standardized Uptake Values, Metabolic Volumes, and Total Lesion Glycolysis. Journal of Nuclear Medicine, 2014, 55, 414-422.	5.0	311
76	Relationship between Tumor Heterogeneity Measured on FDG-PET/CT and Pathological Prognostic Factors in Invasive Breast Cancer. PLoS ONE, 2014, 9, e94017.	2.5	133
77	4DCVF : segmentation variationnelle pour images 3D multicomposantes. Traitement Du Signal, 2014, 31, 9-38.	1.3	0
78	Prognostic implications of volume-based measurements on FDG PET/CT in stage III non-small-cell lung cancer after induction chemotherapy. European Journal of Nuclear Medicine and Molecular Imaging, 2013, 40, 668-676.	6.4	31
79	Comparison of PET metabolic indices for the early assessment of tumour response in metastatic colorectal cancer patients treated by polychemotherapy. European Journal of Nuclear Medicine and Molecular Imaging, 2013, 40, 166-174.	6.4	28
80	Optimized spectral clustering for segmentation of dynamic PET images. , 2013, , .		0
81	Vector-based active surfaces for segmentation of dynamic PET images. , 2013, , .		4
82	Theme B: Biomedical signal and image processing. Irbm, 2013, 34, 6-8.	5.6	0
83	Experimental and analytical comparative study of optical coefficient of fresh and frozen rat tissues. Journal of Biomedical Optics, 2013, 18, 117010.	2.6	56
84	PET-based dose delivery verification in proton therapy: a GATE based simulation study of five PET system designs in clinical conditions. Physics in Medicine and Biology, 2013, 58, 6867-6885.	3.0	21
85	Evaluation of Quantitative Criteria for Glioma Grading With Static and Dynamic 18F-FDopa PET/CT. Clinical Nuclear Medicine, 2013, 38, 81-87.	1.3	32
86	Hybrid GATE: A GPU/CPU implementation for imaging and therapy applications. , 2012, , .		6
87	Optical imaging simulation using GATE. , 2012, , .		1
88	Nonsupervised Ranking of Different Segmentation Approaches: Application to the Estimation of the Left Ventricular Ejection Fraction From Cardiac Cine MRI Sequences. IEEE Transactions on Medical Imaging, 2012, 31, 1651-1660.	8.9	27
89	Realistic and Efficient Modeling of Radiotracer Heterogeneity in Monte Carlo Simulations of PET Images With Tumors. IEEE Transactions on Nuclear Science, 2012, 59, 113-122.	2.0	11
90	A review of partial volume correction techniques for emission tomography and their applications in neurology, cardiology and oncology. Physics in Medicine and Biology, 2012, 57, R119-R159.	3.0	381

#	Article	IF	CITATIONS
91	Lesion-based detection of early chemosensitivity using serial static FDG PET/CT in metastatic colorectal cancer. European Journal of Nuclear Medicine and Molecular Imaging, 2012, 39, 1628-1634.	6.4	10
92	Quantitative Image Analysis in Tomography. , 2012, , 1043-1063.		0
93	Design of Molecular Imaging Systems Assisted by the Monte Carlo Methods. Series in Medical Physics and Biomedical Engineering, 2012, , 273-286.	0.1	0
94	GATE. Series in Medical Physics and Biomedical Engineering, 2012, , 129-152.	0.1	0
95	Nouvelle méthode de segmentation des volumes d'intérêt en TEPÂ: utilisation de la théorie des possibilités. Irbm, 2011, 32, 351-362.	5.6	2
96	Quantification in oncologic FDG-PET: A scientific overview. Medecine Nucleaire, 2011, 35, 320-321.	0.2	0
97	Optimization of a parallel hole collimator/CdZnTe gammaâ€camera architecture for scintimammography. Medical Physics, 2011, 38, 1806-1819.	3.0	21
98	Review and current status of SPECT scatter correction. Physics in Medicine and Biology, 2011, 56, R85-R112.	3.0	146
99	Comparison of different segmentation approaches without using gold standard. Application to the estimation of the left ventricle ejection fraction from cardiac cine MRI sequences. , 2011, 2011, 2663-6.		3
100	Searching for Alternatives to Full Kinetic Analysis in <sup>18</sup> F-FDG PET: An Extension of the Simplified Kinetic Analysis Method. Journal of Nuclear Medicine, 2011, 52, 634-641.	5.0	9
101	Detection and Characterization of Tumor Changes in <sup>18</sup> F-FDG PET Patient Monitoring Using Parametric Imaging. Journal of Nuclear Medicine, 2011, 52, 354-361.	5.0	28
102	Comparison of Bootstrap Resampling Methods for 3-D PET Imaging. IEEE Transactions on Medical Imaging, 2010, 29, 1442-1454.	8.9	33
103	Comparative Assessment of Methods for Estimating Tumor Volume and Standardized Uptake Value in <sup>18</sup> F-FDG PET. Journal of Nuclear Medicine, 2010, 51, 268-276.	5.0	136
104	Simulation-based evaluation and optimization of a new CdZnTe gamma-camera architecture (HiSens). Physics in Medicine and Biology, 2010, 55, 2709-2726.	3.0	28
105	A Preliminary Study of Quantitative Protocols in Indium 111 SPECT Using Computational Simulations and Phantoms. IEEE Transactions on Nuclear Science, 2010, 57, 1096-1104.	2.0	11
106	MultidimensionalB-spline parameterization of the detection probability of PET systems to improve the efficiency of Monte Carlo simulations. Physics in Medicine and Biology, 2010, 55, 3339-3361.	3.0	3
107	LuCaS2: Efficient Monte Carlo simulations of serial PET scans for assessing detection and quantification methods used in patient monitoring. , 2009, , .		2
108	Multidimensional B-spline parameterization of the detection probability of the PET scanner Biograph 16 using GATE. , 2009, , .		1

#	Article	IF	CITATIONS
109	Efficient simulations of iodine 131 SPECT scans using GATE. , 2009, , .		2
110	Introducing improved voxel navigation and fictitious interaction tracking in GATE for enhanced efficiency. Physics in Medicine and Biology, 2009, 54, 2163-2178.	3.0	30
111	Monte Carlo Simulations in Nuclear Medicine Imaging. , 2009, , 177-209.		4
112	Optimization of photon tracking in GATE. , 2008, , .		3
113	Simulation-based evaluation of OSEM iterative reconstruction methods in dynamic brain PET studies. NeuroImage, 2008, 39, 359-368.	4.2	77
114	LuCaS: Efficient Monte Carlo simulations of highly realistic PET tumor images. , 2008, , .		6
115	Comparison Between 2D and 3D Dosimetry Protocols in <sup>90</sup> Y-lbritumomab Tiuxetan Radioimmunotherapy of Patients with Non-Hodgkin's Lymphoma. Cancer Biotherapy and Radiopharmaceuticals, 2008, 23, 53-64.	1.0	24
116	Reply: Feasibility of Automated Partial-Volume Correction of SUVs in Current PET/CT Scanners: Can Manufacturers Provide Integrated, Ready-to-Use Software?. Journal of Nuclear Medicine, 2008, 49, 1032-1033.	5.0	2
117	Impact of Image-Space Resolution Modeling for Studies with the High-Resolution Research Tomograph. Journal of Nuclear Medicine, 2008, 49, 1000-1008.	5.0	217
118	Assigning statistical significance to tumor changes in patient monitoring using FDG pet. , 2008, , .		0
119	Primary Tumor Standardized Uptake Value (SUVmax) Measured on Fluorodeoxyglucose Positron Emission Tomography (FDG-PET) is of Prognostic Value for Survival in Non-small Cell Lung Cancer (NSCLC): A Systematic Review and Meta-Analysis (MA) by the European Lung Cancer Working Party for the IASLC Lung Cancer Staging Project. Journal of Thoracic Oncology, 2008, 3, 6-12.	1.1	466
120	Partial-Volume Effect in PET Tumor Imaging. Journal of Nuclear Medicine, 2007, 48, 932-945.	5.0	1,227
121	Impact of the choice of functional regions in targeted fully 3D SPECT reconstruction. , 2007, , .		1
122	Fully 4D image reconstruction by estimation of an input function and spectral coefficients. , 2007, , .		33
123	Fully 4D reconstruction applied to respiratory gated PET acquisitions. , 2007, , .		0
124	Simulation-based evaluation of NEG-ML iterative reconstruction of low count PET data. , 2007, , .		12
125	Quantification in emission tomography: Challenges, solutions, and performance. Nuclear Instruments and Methods in Physics Research, Section A: Accelerators, Spectrometers, Detectors and Associated Equipment, 2007, 571, 10-13.	1.6	11
126	Accuracy of partial volume effect correction in clinical molecular imaging of dopamine transporter using SPECT. Nuclear Instruments and Methods in Physics Research, Section A: Accelerators, Spectrometers, Detectors and Associated Equipment, 2007, 571, 173-176.	1.6	5

#	Article	IF	CITATIONS
127	Iterative Kinetic Parameter Estimation within Fully 4D PET Image Reconstruction. , 2006, , .		23
128	Simulation-based Evaluation of Iterative Reconstructions in Dynamic [18F]MPPF PET studies. , 2006, , .		0
129	Targeted Fully 3D Monte Carlo Reconstruction in SPECT. , 2006, , .		5
130	Fully 3D Monte Carlo image reconstruction in SPECT using functional regions. Nuclear Instruments and Methods in Physics Research, Section A: Accelerators, Spectrometers, Detectors and Associated Equipment, 2006, 569, 399-403.	1.6	21
131	Partial volume effect correction in SPECT for striatal uptake measurements in patients with neurodegenerative diseases: impact upon patient classification. European Journal of Nuclear Medicine and Molecular Imaging, 2006, 33, 1062-1072.	6.4	39
132	Monte Carlo simulations in emission tomography and GATE: An overview. Nuclear Instruments and Methods in Physics Research, Section A: Accelerators, Spectrometers, Detectors and Associated Equipment, 2006, 569, 323-329.	1.6	77
133	Assessment of the Mosaic animal PET system response using list-mode data for validation of GATE Monte Carlo modelling. Nuclear Instruments and Methods in Physics Research, Section A: Accelerators, Spectrometers, Detectors and Associated Equipment, 2006, 569, 220-224.	1.6	11
134	Simultaneous Estimation of Temporal Basis Functions and Fully 4D PET Images. , 2006, , .		5
135	Clinical comparison of HiRez versus non-HiRez LSO crystal sampling for lesion detection and SUV quantification. , 2006, , .		0
136	Joint estimation of dynamic PET images and temporal basis functions using fully 4D ML-EM. Physics in Medicine and Biology, 2006, 51, 5455-5474.	3.0	86
137	Quantification in simultaneous99mTc/123I brain SPECT using generalized spectral factor analysis: a Monte Carlo study. Physics in Medicine and Biology, 2006, 51, 6157-6171.	3.0	18
138	Unified description and validation of Monte Carlo simulators in PET. Physics in Medicine and Biology, 2005, 50, 329-346.	3.0	33
139	From Anatomic Standardization Analysis of Perfusion SPECT Data to Perfusion Pattern Modeling. Academic Radiology, 2005, 12, 554-565.	2.5	10
140	Monte Carlo simulation in PET and SPECT instrumentation using GATE. Nuclear Instruments and Methods in Physics Research, Section A: Accelerators, Spectrometers, Detectors and Associated Equipment, 2004, 527, 180-189.	1.6	80
141	Feasibility and value of fully 3D Monte Carlo reconstruction in single-photon emission computed tomography. Nuclear Instruments and Methods in Physics Research, Section A: Accelerators, Spectrometers, Detectors and Associated Equipment, 2004, 527, 195-200.	1.6	13
142	Diffusion regularization for iterative reconstruction in emission tomography. IEEE Transactions on Nuclear Science, 2004, 51, 712-718.	2.0	11
143	Evaluation of Registration of Ictal SPECT/MRI Data Using Statistical Similarity Methods. Lecture Notes in Computer Science, 2004, , 687-695.	1.3	3
144	From Anatomic Standardization Analysis of Perfusion SPECT Data to Perfusion Pattern Modelling. Lecture Notes in Computer Science, 2003, , 328-335.	1.3	2

#	Article	IF	CITATIONS
145	Quantitative accuracy of dopaminergic neurotransmission imaging with (123)I SPECT. Journal of Nuclear Medicine, 2003, 44, 1184-93.	5.0	80
146	Biases affecting the measurements of tumor-to-background activity ratio in PET. IEEE Transactions on Nuclear Science, 2002, 49, 2112-2118.	2.0	19
147	A non-parametric bootstrap approach for analysing the statistical properties of SPECT and PET images. Physics in Medicine and Biology, 2002, 47, 1761-1775.	3.0	58
148	Iterative reconstruction of SPECT data with adaptive regularization. IEEE Transactions on Nuclear Science, 2002, 49, 2350-2354.	2.0	80
149	Comparison of four scatter correction methods for patient whole-body imaging during therapeutic trials with iodine-131. Cancer, 2002, 94, 1224-1230.	4.1	10
150	Importance of the choice of the collimator for the detection of small lesions in scintimammography: a phantom study. Physics in Medicine and Biology, 2001, 46, 1343-1355.	3.0	15
151	A Methodology to Validate MRI/SPECT Registration Methods Using Realistic Simulated SPECT Data. Lecture Notes in Computer Science, 2001, , 275-282.	1.3	14
152	Should scatter be corrected in both transmission and emission data for accurate quantitation in cardiac SPET?. European Journal of Nuclear Medicine and Molecular Imaging, 2000, 27, 1356-1364.	2.1	4
153	Respective roles of scatter, attenuation, depth-dependent collimator response and finite spatial resolution in cardiac single-photon emission tomography quantitation: a Monte Carlo study. European Journal of Nuclear Medicine and Molecular Imaging, 1999, 26, 437-446.	6.4	31
154	Quantitation in planar renal scintigraphy: which µ value should be used?. European Journal of Nuclear Medicine and Molecular Imaging, 1999, 26, 1610-1613.	6.4	2
155	<title>The need to develop guidelines for the evaluation of medical image processing procedures</title> . , 1999, 3661, 1466.		11
156	Testing observer's ability to detect if an image was compressed shows large observer variability. , 1999, 3658, 538.		0
157	Implications of dual-energy-window (DEW) scatter correction inaccuracies for 111In quantitative geometric mean imaging. Nuclear Medicine Communications, 1997, 18, 79-86.	1.1	4
158	Measurement of Myocardial Wall Thickening from PET/SPECT Images: Comparison of Two Methods. Journal of Computer Assisted Tomography, 1996, 20, 473-481.	0.9	15
159	Realignment of Emission Contaminated Attenuation Maps with Uncontaminated Attenuation Maps for Attenuation Correction in PET. Journal of Computer Assisted Tomography, 1996, 20, 848-854.	0.9	3
160	Attenuation correction in cardiac positron emission tomography and single-photon emission computed tomography. Journal of Nuclear Cardiology, 1995, 2, 246-255.	2.1	27
161	A comparative study of scatter correction methods for scintigraphic images. European Journal of Nuclear Medicine and Molecular Imaging, 1994, 21, 388-393.	2.1	12
162	Scatter correction in scintigraphy: the state of the art. European Journal of Nuclear Medicine and Molecular Imaging, 1994, 21, 675-694.	2.1	81

#	Article	IF	CITATIONS
163	Foundations of factor analysis of medical image sequences: a unified approach and some practical implications. Image and Vision Computing, 1994, 12, 375-385.	4.5	22
164	<title>Statistical model for tomographic reconstruction methods using spline functions</title> . , 1994, , .		5
165	<title>CAMIS: clustering algorithm for medical image sequences using a mutual nearest neighbor criterion</title> . , 1994, 2299, 336.		2
166	Extraction of functional volumes from medical dynamic volumetric data sets. Computerized Medical Imaging and Graphics, 1993, 17, 397-404.	5.8	19
167	<title>Optimal metric for factor analysis of medical image sequences</title> . , 1993, , .		0